The EMBO Journal (2006) 25, 4468–4478 | © 2006 European Molecular Biology Organization | All Rights Reserved 0261-4189/06
www.embojournal.org

THE EMBO JOURNAL

PtdIns3P binding to the PX domain of p40^{phox} is a physiological signal in NADPH oxidase activation

Chris Ellson[1], Keith Davidson[1], Karen Anderson[1], Len R Stephens[2] and Phillip T Hawkins[2,*]

Inositide Laboratory, The Babraham Institute, Babraham Research Campus, Cambridge, UK

The production of reactive oxygen species by the NADPH oxidase complex of phagocytes plays a critical role in our defence against bacterial and fungal infections. The PX domains of two oxidase components, p47^{phox} and p40^{phox}, are known to bind phosphoinositide products of PI3Ks but the physiological roles of these interactions are unclear. We have created mice which carry an R58A mutation in the PX domain of their p40^{phox} gene, which selectively prevents binding to PtdIns3P. p40$^{phoxR58A/R58A}$ embryos do not develop normally but p40$^{phoxR58A/-}$ mice are viable and neutrophils from these animals exhibit significantly reduced oxidase responses compared to those from their p40$^{phox+/-}$ siblings (e.g. 60% reduced in response to phagocytosis of *Staphylococcus aureus*). Wortmannin inhibition of the *S. aureus* oxidase response correlates with inhibition of phagosomal PtdIns3P accumulation and overlaps with the reduction in this response caused by the R58A mutation, suggesting PI3K regulation of this response is substantially dependent on PtdIns3P-binding to p40^{phox}. p40$^{phoxR58A/-}$ mice are significantly compromised in their ability to kill *S. aureus in vivo*, defining the physiological importance of this interaction.

The EMBO Journal (2006) **25,** 4468–4478. doi:10.1038/sj.emboj.7601346; Published online 21 September 2006
Subject Categories: signal transduction; immunology
Keywords: NADPH oxidase; p40^{phox}; PI3K; PtdIns3P; PX domain

Introduction

The NADPH oxidase in phagocytic cells, such as neutrophils and macrophages, plays a key role in our innate immune system (Nathan, 2006). This oxidase is a multisubunit enzyme complex that transfers electrons from NADPH, across the membrane on which it is assembled, to molecular oxygen (Cross and Segal, 2004; Quinn and Gauss, 2004; Sheppard *et al*, 2005). The superoxide anions (O_2^-) thus formed can then be converted, depending on their location, by both enzymatic and non-enzymatic routes to a variety of other reactive oxygen species (ROS) and halide derivatives (e.g. HOCl). This transfer of electrons is electrogenic and there is much debate over the nature of the compensating currents, which must occur to allow significant quantities of ROS to be generated, with evidence to suggest both H^+ and K^+ channels are involved (Cross and Segal, 2004; Murphy and DeCoursey, 2006). It is thought that a compensating K^+ current generated by NADPH oxidase activity on phagosomal membranes leads to substantial accumulation of K^+ inside the phagosome, leading to subsequent activation of several proteases (Reeves *et al*, 2002), which, together with the toxicity of the ROS and halide derivatives themselves, plays a key role in the killing of pathogens in this organelle (Hampton *et al*, 1998). The importance of the NADPH oxidase in the killing of several species of bacteria and fungi, in particular, is clear from the recurrent, life-threatening infections, which occur in chronic granulamatous disease (CGD), a condition caused by germ line mutations in several of the oxidase subunits (Meischl and Roos, 1998; Heyworth *et al*, 2003).

Analysis of the nature of the mutations in CGD, together with classical biochemical purification and *in vitro* reconstitution, has defined a core set of components sufficient for NADPH oxidase activity, these include a two subunit, membrane bound cytochrome b_{558} (gp91^{phox} and p22^{phox}) and three soluble components, p67^{phox}, p47^{phox} and GTP-rac (Cross and Segal, 2004; Quinn and Gauss, 2004). Additionally, p67^{phox} is known to bind tightly to another oxidase subunit, p40^{phox} (Matute *et al*, 2005). The function of p40^{phox} has been unclear; no mutations in p40^{phox} have been found to cause CGD, heterologous expression of this protein in model cell systems has been shown to both promote and inhibit oxidase activity in response to different agonists and *in vitro* reconstitution experiments have suggested p40^{phox} has a positive or neutral role in NADPH oxidase activation (Matute *et al*, 2005). We have recently created p40$^{phox-/-}$ mice and reported large reductions in oxidase responses to a variety of agonists in their bone marrow-derived neutrophils (Ellson *et al*, 2006). However, these mice also show substantial reductions in the expression of p67^{phox} (approx. 55% reduced) which, given the established importance of p67^{phox} in the catalytic mechanism of the oxidase, makes it difficult to accurately ascribe a role for p40^{phox} alone in these responses. The scale of the reductions in oxidase activation in p40$^{phox-/-}$ neutrophils to some phagocytic stimuli (e.g. 85% reduced in response to *Staphylococcus aureus* and IgG-latex beads) (Ellson *et al*, 2006), together with recent data describing a clear dependency of an IgG-SRBC-induced oxidase burst on heterologous expression of p40^{phox} in Cos^{phox} cells (Suh *et al*, 2006), indicates p40^{phox} is likely to have an important role, at least, in the assembly of an active NADPH oxidase on phagosomes.

Many different cell surface receptors are able to regulate the neutrophil's NADPH oxidase activity at sites of infection

*Corresponding author. Inositide Laboratory, The Babraham Institute, Babraham Research Campus, Cambridge CB2 4AT, UK.
Tel: +44 1223 496598; Fax: +44 1223 496043;
E-mail: phillip.hawkins@bbsrc.ac.uk
[1]These authors contributed equally to this work
[2]These authors contributed equally to this work

Received: 25 June 2006; accepted: 18 August 2006; published online: 21 September 2006

and inflammation. These include receptors for opsonin coats (e.g. Fcγ receptors and integrins for antibodies or complement, respectively), the so-called pattern receptors for complex molecules exposed on the surface of microbes themselves and also a range of soluble inflammatory stimuli, such as combinations of chemokines and cytokines found at sites of inflammation (e.g. fMLP and TNFα) (Sheppard *et al*, 2005). Hence, the signalling pathways that couple this array of cell surface receptors to activation of the NADPH oxidase complex are necessarily complex, with evidence to suggest many different, interacting, signalling pathways are involved, for example PLC, PI3K, PLD, PLA_2, MAPKs (Quinn and Gauss, 2004; Sheppard *et al*, 2005). At the level of the oxidase, key events are thought to be multiple phosphorylation of the C-terminus of $p47^{phox}$, which relieves an intramolecular SH3 domain/C-terminus constraint, allowing interaction with $p22^{phox}$ (Faust *et al*, 1995; Perisic *et al*, 2004; Groemping and Rittinger, 2005). Further, GTP/GDP exchange on Rac promotes complex formation with $p67^{phox}$ and $gp91^{phox}$ (Lapouge *et al*, 2000; Diebold and Bokoch, 2001; Perisic *et al*, 2004). Thus, through a series of mutual contacts, complex formation between soluble and membrane bound oxidase components is promoted at a particular membrane location, allowing efficient transfer of electrons from NADPH to O_2. There is still much to be done, however, in identifying which signalling molecules are responsible for delivering this regulation downstream of defined receptors and, in particular, the relative balance of their contributions in what must be a robust, and hence probably redundant, signalling web to this important component of our innate immune response.

There has been much interest in the role of PI3K signalling pathways in NADPH oxidase regulation. Wortmannin, a relatively specific and broad range catalytic inhibitor of PI3Ks, is a potent inhibitor of neutrophil oxidase responses to a variety of stimuli and mice deficient in the PI3Kγ isoform exhibit dramatically reduced oxidase responses to activation of Gi-coupled receptors on neutrophils (Perisic *et al*, 2004). There is good evidence that receptor-stimulated class I PI3Ks generate PtdIns(3,4,5)P_3 in neutrophil plasma membranes, which can subsequently activate guanine nucleotide exchange factors for Rac2 (Vav and P-Rex families), allowing regulation of a Rac2-dependent input into NADPH oxidase activation (Dinauer, 2003; Welch *et al*, 2003, 2005; Dong *et al*, 2005). There is also good evidence that phosphoinositide products of PI3Ks can bind directly to the PX domains of the oxidase subunits $p47^{phox}$ and $p40^{phox}$ (Ago *et al*, 2001; Ellson *et al*, 2001a; Kanai *et al*, 2001; Karathanassis *et al*, 2002; Perisic *et al*, 2004). The binding of PtdIns3P to the PX domain of $p40^{phox}$ is, in particular, of sufficient affinity and specificity to suggest it must play a physiological role in the regulation of $p40^{phox}$ function. Further, a crystal structure for short-chain PtdIns3P bound to the isolated PX domain of this molecule is available (Bravo *et al*, 2001), which provides an opportunity to test this role through specific mutagenesis. PtdIns3P is an established product of class III PI3K activity in the endosomal system of eukaryotic cells but has more recently been shown also to accumulate on phagosomal membranes, shortly after fission from the plasma membrane (Vieira *et al*, 2001; Ellson *et al*, 2001b). Hence, it appeared plausible that PtdIns3P might act as a signalling molecule, which regulates NADPH oxidase activity at this location via binding to $p40^{phox}$. We generated mice expressing a version of $p40^{phox}$ carrying a single point mutation in its PX domain, which prevents binding to PtdIns3P, to test this hypothesis.

Results

Generation of $p40^{phoxR58/-}$ mice

We generated two independent ES cell lines each possessing one $p40^{phoxR58A}$ allele. The targeting strategy introduced a single codon change in exon 3, resulting in conversion of arginine at amino-acid position 58 to alanine (Figure 1). Mutation of R58 (to either Q or A) has been demonstrated to prevent PtdIns3P binding to the PX domain of $p40^{phox}$ (Bravo *et al*, 2001; Zhan *et al*, 2002), with minimal predicted changes to the overall fold of the protein (Bravo *et al*, 2001).

These two ES cell lines were used to generate male chimeras via blastocyst injection and $p40^{phoxR58A/+}$ heterozygotes were created by breeding with $C57^{BL/6}$ females. The 'floxed' neomycin resistance cassette introduced into the intron between exons 3 and 4 (Figure 1) was removed at this stage via Cre-mediated excision in the testes (see Materials and methods). Interbreeding of the $p40^{phoxR58/+}$ heterozygotes generated further $p40^{phox+/+}$ and $p40^{phoxR58/+}$ animals, but only approximately 1 in 50 predicted $p40^{phoxR58A/R58A}$ live births (Table I). Further analysis of 70 embryos derived from timed matings indicated $p40^{phoxR58A/R58A}$ embryos failed in development before day 10 (data not shown).

Breeding $p40^{phox-/-}$ mice with $p40^{phoxR58A/+}$ heterozygotes generated $p40^{phox+/-}$ and $p40^{phoxR58A/-}$ mice in the expected 1:1 ratio (Table I), indicating that embryonic lethality requires two copies of the $p40^{phoxR58A}$ allele. Importantly, comparison of the $p40^{phox+/-}$ and $p40^{phoxR58A/-}$ siblings allows a direct comparison of the protein products of $p40^{phoxR58A}$ and $p40^{phox+}$ alleles.

$p40^{phoxR58A/-}$ mice were apparently normal, healthy and fertile when kept under pathogen-controlled conditions. Blood cell counts from $p40^{phoxR58A/-}$ mice were normal (Figure 2A) and bone marrow derived neutrophils (BMNs) from $p40^{phoxR58A/-}$ mice exhibited normal differentiated phenotypes with respect to their morphology and phagocytosis of bacteria, zymosan and IgG-latex beads (data not shown and see below). $p40^{phoxR58A/-}$ neutrophils showed comparable expression of $p47^{phox}$ and, importantly, $p67^{phox}$ (Figure 2B and D). R58A-$p40^{phox}$ protein itself exhibited a slightly retarded mobility on SDS–PAGE and was expressed at a slightly greater level in $p40^{phoxR58A/-}$ neutrophils than wild-type $p40^{phox}$ in $p40^{phox+/-}$ neutrophils (Figure 2B and C).

$p40^{phoxR58A/-}$ neutrophils exhibit significant reductions in ROS production in response to TNFα/fMLP and IgG-latex beads

Several soluble inflammatory stimuli (e.g. fMLP, PAF, LTB4) are known to induce the assembly of the NADPH oxidase at the plasma membrane and the generation of extracellular ROS. The responses to these stimuli are characteristically augmented by prior exposure to the so-called 'priming' cytokines (e.g. GM-CSF, TNFα), a phenomenon thought to localise the production of potentially self-damaging ROS to sites of inflammation (Hallett and Lloyds, 1995; Sheppard *et al*, 2005). We measured the generation of ROS in response to fMLP in TNF-α primed, BMNs from $p40^{phoxR58A/-}$ and $p40^{phox+/-}$ mice using a luminol-dependent, chemiluminescence assay

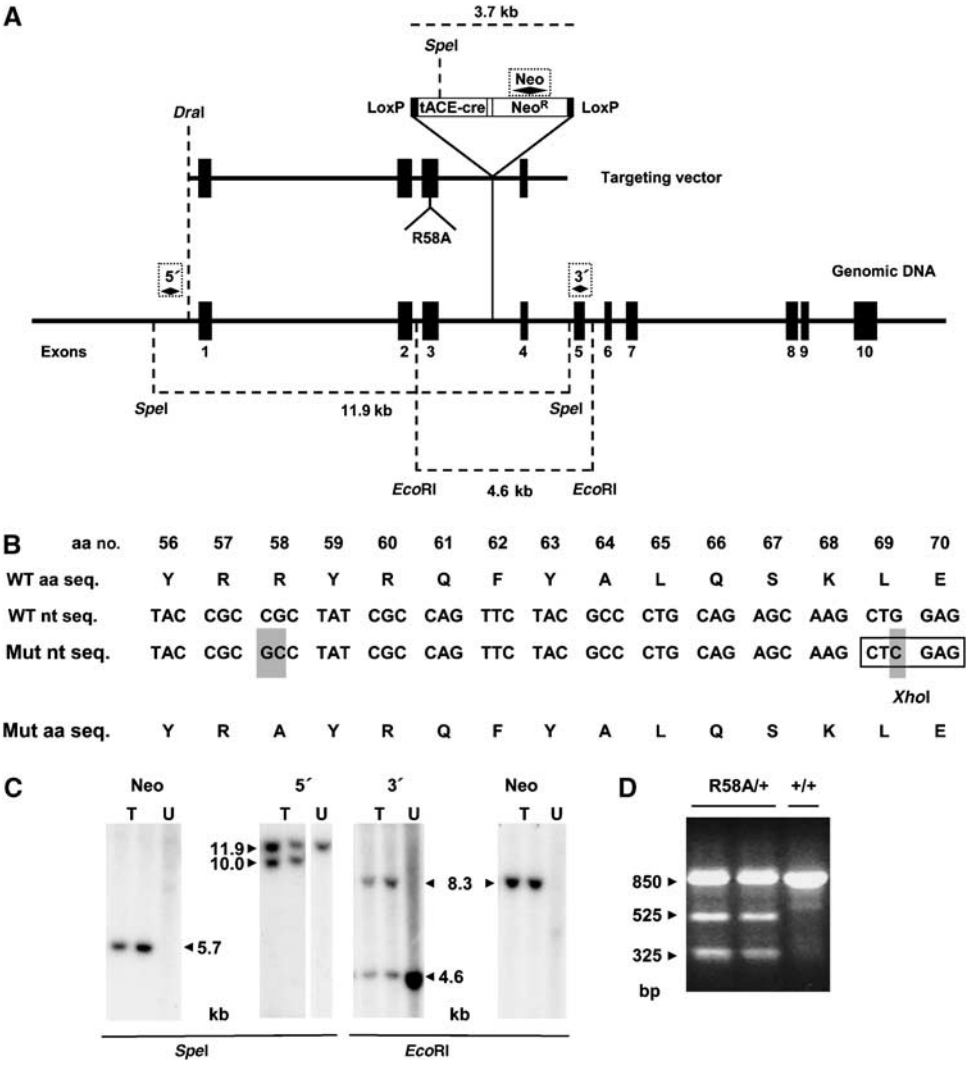

Figure 1 p40^{phoxR58A} targeting strategy. (**A**) Schematic of p40^{phoxR58A} targeting strategy. The intron–exon structure of the p40^{phox} gene (*ncf4*), the extent and overall organisation of the targeting construct, and relevant restriction sites and fragment sizes are shown. Positions of Southern blot probes are shown as diamonds in dotted boxes. Drawing not to scale. (**B**) Mutations introduced by the targeting strategy are highlighted. (**C**) Examples of Southern blots of ES cell DNA digested with *Spe*I or *Eco*RI and probed with the Neo, 5′ or 3′ probes. T, targeted; U, untargeted. (**D**) Example of PCR screening of mouse tail genomic DNA of progeny from p40$^{phoxR58A/+}$ matings. Primers flanking exon 3 generate an 850 bp fragment that is *Xho*I-cleaved to 525 and 325 bp in targeted alleles.

Table I Number of live births from interbreeding p40$^{phoxR58A/+}$ heterozygotes, derived from two independent ES cell lines, and subsequent breeding of p40$^{phoxR58A/+}$ heterozygotes offspring with p40$^{phox-/-}$ homozygous mice

Genotype of offspring	ES cell line (EB6) p40$^{phoxR58A/+}$ × p40$^{phoxR58A/+}$	ES cell line (GA4) p40$^{phoxR58A/+}$ × p40$^{phoxR58A/+}$	p40$^{phoxR58A/+}$ × p40$^{phox-/-}$
+/+	53	36	
R58A/+	100	88	
R58A/R58A	1	1	
+/−			77
R58A/−			59
Total	154	125	136

in the presence of horse radish peroxidise (HRP), an assay that provides a sensitive, rate-measure of extracellular ROS production (Dahlgren and Karlsson, 1999). The kinetics of these responses in the p40$^{phoxR58A/-}$ and p40$^{phox+/-}$ neutrophils were very similar but the total ROS accumulated in the p40$^{phoxR58A/-}$ neutrophils was reduced by about 19% (Figure 3A).

It is well established that neutrophils undergoing FcγR-mediated phagocytosis of IgG-coated particles assemble an active NADPH oxidase at the phagosome (Zhou and Brown, 1994; Jakus *et al*, 2004; Ueyama *et al*, 2004). We measured the generation of intracellular ROS in primed, BMNs from p40$^{phoxR58A/-}$ and p40$^{phox+/-}$ mice in response to uptake of IgG-latex beads using luminol-dependent chemiluminescence in the absence of added HRP. This assay provides a rate measure of intracellular ROS production in the vicinity of endogenous peroxidases, which previous work has indicated is dictated under these conditions by co-incidental release of ROS and myeloperoxidase into the phagosome (Dahlgren and Karlsson, 1999). Intracellular ROS production in response to phagocytosis of IgG-latex beads was substantially reduced in p40$^{phoxR58A/-}$ neutrophils compared to p40$^{phox+/-}$ neutrophils (approximately 42% reduction; Figure 3B).

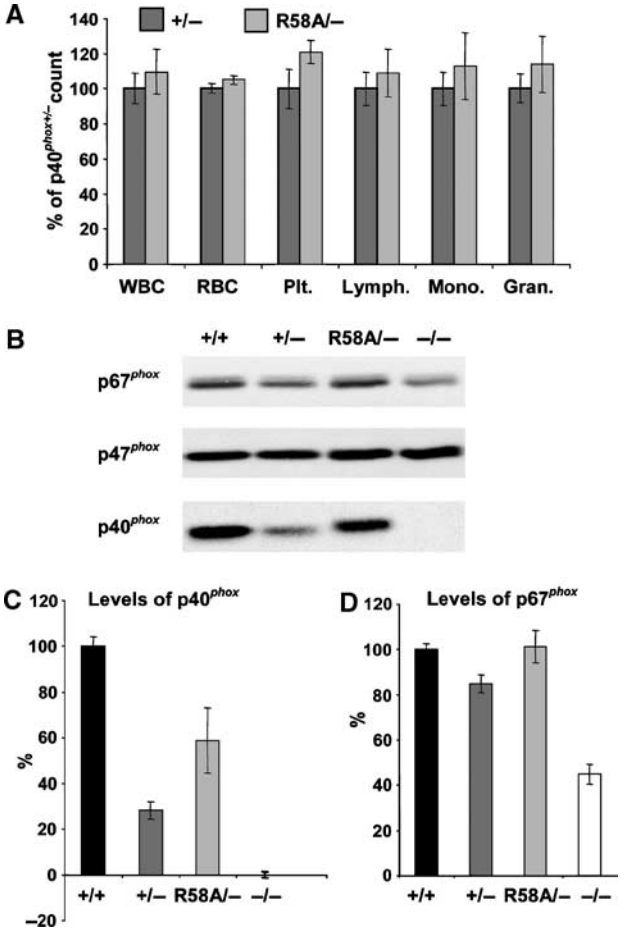

Figure 2 Blood cell counts and phox protein expression in $p40^{phoxR58A/-}$ mice. (**A**) Blood cell counts from $p40^{phox+/-}$ and $p40^{phoxR58A/-}$ animals (WBC, white blood cells; RBC, red blood cells; Plt, platelets, Lymph, lymphocytes; Mono, monocytes; Gran, granulocytes). Data represented are mean % of $p40^{phox+/-}$ counts ± s.e. ($n = 12$). (**B**–**D**) BMNs from $p40^{phox+/+}$, $^{+/-}$, $^{R58A/-}$ and $^{-/-}$ animals were sonicated into SDS sample buffer, subjected to SDS–PAGE and immunoblotted for $p40^{phox}$, $p47^{phox}$ and $p67^{phox}$. Graphs represent mean % of $p40^{phox+/+}$ samples ± s.e. ($n = 10$–13) from four independent experiments, using 3–6 mice per preparation.

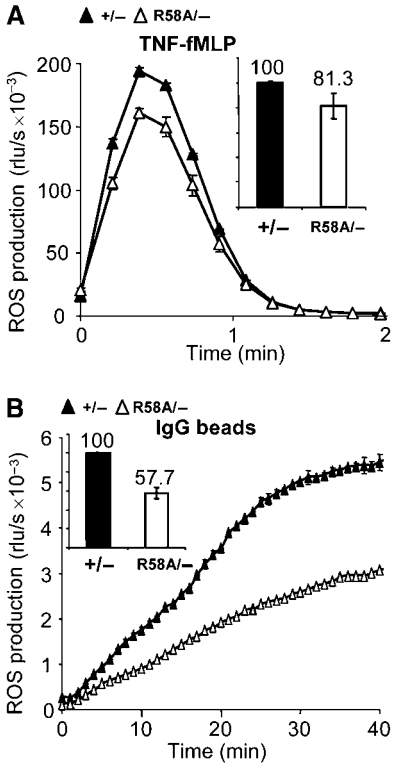

Figure 3 $p40^{phoxR58A/-}$ neutrophils have defects in ROS production in response to TNFα/fMLP and IgG-latex beads. Duplicate wells of BMNs were stimulated in a luminometer and ROS production was followed over time. Response kinetics (line graph; mean ± range of one representative experiment), and total integrated responses as % of $p40^{phox+/-}$ (bar graph; mean ± s.e.; $n = 22$ from 11 independent experiments, and $n = 11$ from five independent experiments for TNFα/fMLP and IgG-latex beads, respectively). (**A**) fMLP-stimulated production of extracellular ROS in mTNFα-primed BMNs from $p40^{phoxR58A/-}$ and $^{+/-}$ animals. (**B**) IgG-latex bead-stimulated production of intracellular ROS in primed BMNs from $p40^{phox+/-}$ and $p40^{phoxR58A/-}$ animals.

Phagocytosis itself was not influenced by the R58A mutation (data not shown), indicating a specific signalling defect to NADPH oxidase activation under these circumstances.

$p40^{phoxR58A/-}$ neutrophils exhibit a large reduction in intracellular ROS production in response to S. aureus that is equivalent to a large, wortmannin-sensitive element in this response

We measured the production of intracellular ROS in response to phagocytosis of *S. aureus* in primed, BMNs from $p40^{phoxR58A/-}$ and $p40^{phox+/-}$ mice. We observed a large reduction, of about 60%, in this response in $p40^{phoxR58A/-}$ neutrophils (Figure 4A). Phagocytic uptake of *S. aureus* was normal in these neutrophils (Figure 4D) suggesting that, as with the oxidase response to IgG-latex beads, there is a specific defect in the phagosomal oxidase response in neutrophils from $p40^{phoxR58A/-}$ animals.

We also measured the sensitivity of intracellular ROS production in response to *S. aureus*, in both $p40^{phoxR58A/-}$ and $p40^{phox+/-}$ neutrophils, to inhibition by the general PI3K inhibitor wortmannin (Figure 4A). Phagocytosis of *S. aureus* was not significantly inhibited at the concentrations of wortmannin used (Figure 4D), consistent with previous reports that phagocytic uptake of small particles, requiring minimal membrane extension, is relatively insensitive to PI3K inhibition (Cox *et al*, 1999). This allows a window in which the potential for more direct involvement of PI3Ks in this oxidase response can be evaluated.

The inhibition of *S. aureus* oxidase responses by wortmannin was complex. The initial phase of ROS production was substantially inhibited by wortmannin, but an increasingly significant proportion of the total response at later times was insensitive to doses of wortmannin up to 300 nM (Figure 4A), suggesting differential requirement for PI3K signalling in these responses with time. Importantly, the initial phases of ROS production in $p40^{phox+/-}$ and $p40^{phoxR58A/-}$ neutrophils were differentially sensitive to wortmannin inhibition (Figure 4B and C). The R58A mutation did not reduce further the residual ROS response in the presence of 100 nM wortmannin, suggesting the wortmannin-sensitive components in this response are on the same pathway to oxidase activation as the R58A lesion. The initial ROS response in $p40^{phoxR58A/-}$ neutrophils was partially inhibited by low

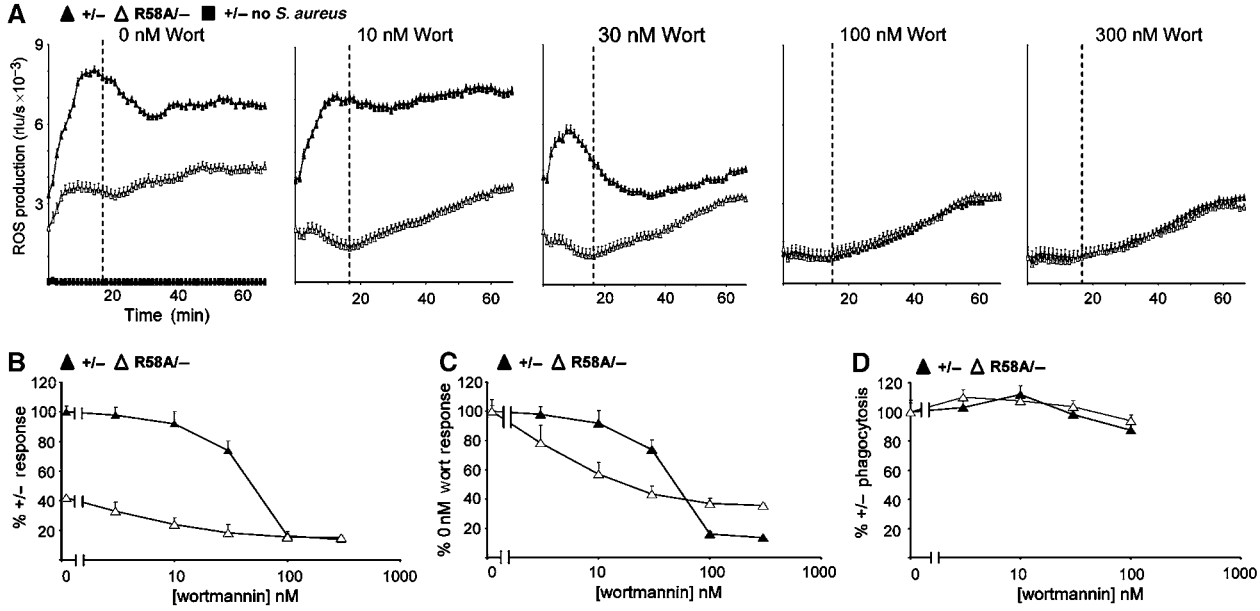

Figure 4 $p40^{phoxR58A/-}$ neutrophils exhibit reduced intracellular ROS production in response to phagocytosis of *S. aureus*, which equates with a wortmannin-sensitive component of the response. Primed BMNs from $p40^{phoxR58A/-}$ and $^{+/-}$ animals were analysed for *S. aureus*-induced intracellular ROS production. Where appropriate, cells were pretreated with indicated wortmannin concentrations for 10 min prior to addition of *S. aureus*. (**A**) Time course of ROS production in the presence of increasing concentrations of wortmannin. Data are means ± s.d. from a single experiment, performed in triplicate, representative of three independent experiments. (**B, C**) Total integrated ROS responses for the first 16.5 min of each condition (as indicated by dashed lines in A) were calculated and expressed as a percentage of $p40^{phox+/-}$ response (B), or as a percentage of relevant control response for $p40^{phox+/-}$ and $p40^{phoxR58A/-}$ (C). Data are mean ± s.e. ($n \geqslant 8$). (**D**) Phagocytosis of *S. aureus* by $p40^{phox+/-}$ and $p40^{phoxR58A/-}$ BMN and the effects of wortmannin. Data shown are mean ± s.e. from at least 100 cells at each condition, expressed as a percentage of $p40^{phox+/-}$ phagocytosis.

doses of wortmannin in the concentration range expected to inhibit Class I PI3K-catalysed generation of PtdIns(3,4,5)P_3 (Figure 4B and C) (Stephens *et al*, 1994; Knight *et al*, 2006). However, the large component of the response in $p40^{phox+/-}$ neutrophils, which is sensitive to inhibition by wortmannin with an IC_{50} of approximately 50 nM, is absent in $p40^{phoxR58A/-}$ neutrophils (Figure 4B and C). This suggests approximately 60% of initial ROS production in response to *S. aureus* requires a pathway ablated both by the R58A mutation and modest doses of wortmannin in the range expected to inhibit Class III/Class IIb-catalysed generation of PtdIns3P after short incubation periods with cells (Stephens *et al*, 1994; M Fry, personal communication, 2006).

$p40^{phoxR58A/-}$ neutrophils exhibit differential reductions in intracellular versus extracellular ROS production in response to PMA

PMA is often used as a receptor-independent stimulus of oxidase assembly and activation. The mechanism of action of PMA in this respect is incompletely understood but must, at least in part, involve PKC-mediated phosphorylation of $p47^{phox}$ (Dekker *et al*, 2000; Dang *et al*, 2001; Fontayne *et al*, 2002; Bey *et al*, 2004). Using chemiluminescent detection methods for ROS, PMA has previously been shown to stimulate a large extracellular production of ROS, which is insensitive to inhibition of PI3Ks and a smaller, intracellular production, which is potently inhibited by wortmannin (Karlsson *et al*, 2000; Brown *et al*, 2003). We used luminol-dependent chemiluminescence in the presence and absence of added HRP to compare the oxidase responses to PMA in neutrophils from $p40^{phoxR58A/-}$ and $p40^{phox+/-}$ mice.

The kinetics of both intracellular and extracellular ROS production in response to PMA are clearly complex with at least two clear phases (Figure 5 and data not shown). We found that both phases of extracellular ROS production in response to PMA were extremely similar in $p40^{phoxR58A/-}$ and $p40^{phox+/-}$ neutrophils (Figure 5A and data not shown). However, the initial phase of intracellular ROS formation in response to PMA was reduced by almost half in neutrophils from the $p40^{phoxR58A/-}$ mice (Figure 5B and C).

As expected, wortmannin had little effect on the release of extracellular ROS but had a significant effect on the production of intracellular ROS (Figure 5). The initial phase of the intracellular ROS response in $p40^{phox+/-}$ neutrophils was inhibited by wortmannin, to a level very similar to that seen in the $p40^{phoxR58A/-}$ neutrophils. Importantly, wortmannin was unable to reduce significantly this phase of the response any further in $p40^{phoxR58A/-}$ neutrophils (Figure 5B and D). These results suggest there is a large component of the initial phase of PMA-stimulated intracellular ROS accumulation that is dependent on PtdIns3P-binding to $p40^{phox}$.

PtdIns3P accumulation and NADPH oxidase activation are inhibited in parallel by wortmanninin

We measured, in parallel, the wortmannin sensitivity of PtdIns3P accumulation on phagosomes and intracellular ROS production in response to uptake of *S. aureus*, in differentiated, human neutrophil-like PLB-985 cells stably expressing a GFP-tagged, isolated PX domain of $p40^{phox}$(GFP-iPX) (Ellson *et al*, 2001b). The presence of the GFP-tagged, PtdIns3P-probe allows a semiquantitative

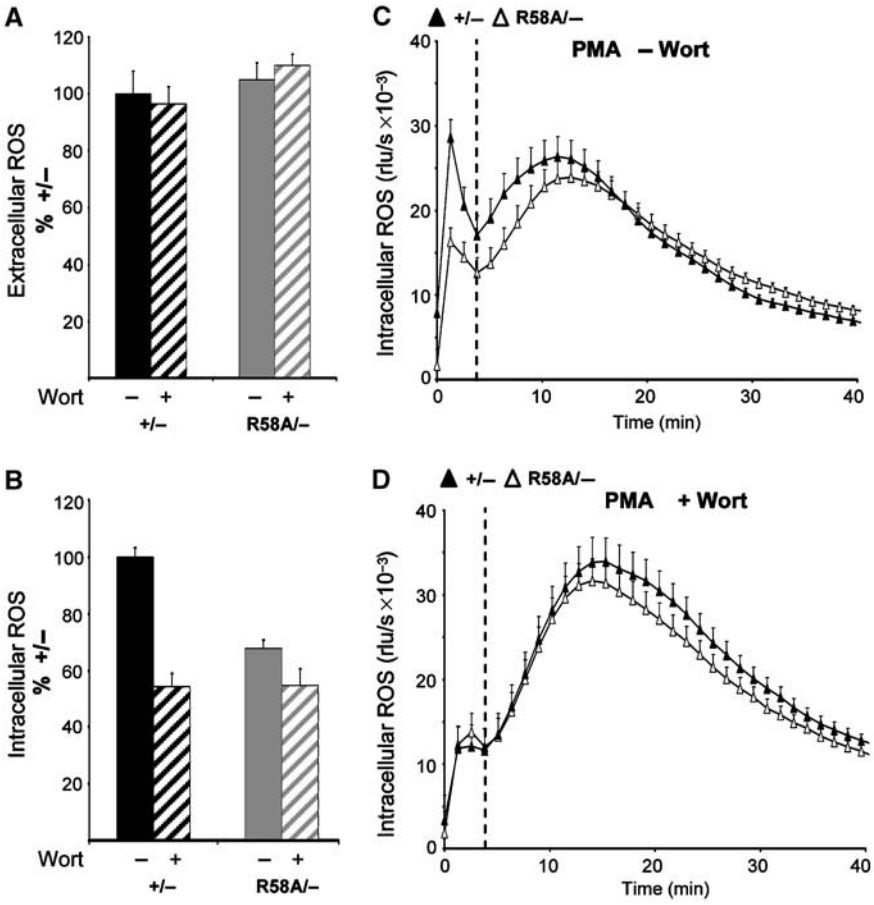

Figure 5 $p40^{phoxR58A/-}$ neutrophils have reductions in intracellular but not extracellular ROS production in response to PMA. Primed BMNs from $p40^{phoxR58A/-}$ and $^{+/-}$ animals were analysed for PMA-induced ROS production, using luminol-dependent chemiluminescence either in the presence of HRP (extracellular, **A**) or absence of HRP (intracellular, **B**–**D**) and either in the presence or absence of wortmannin (100 nM). Kinetics of ROS production are shown as means ± s.d. from a single experiment performed in triplicate, representative of three independent experiments. Total integrated ROS produced during the initial phase of PMA stimulated ROS production (indicated by dashed line in (C, D)) are shown in the bar graphs (A, B) as a percentage of the relevant $p40^{phox+/-}$ response; means ± s.e. ($n = 9$).

measure of PtdIns3P accumulation around *S. aureus*-containing phagosomes (Figure 6). PLB-985 cells expressing GFP-iPX show equivalent oxidase responses to a variety of soluble and particulate stimuli, compared to cells with no exogenous protein expression, suggesting that, at the expression levels achieved, the concentration of the iPX-domain does not influence oxidase activation (data not shown). At the concentrations tested, we observed little effect of wortmannin on the rate of *S. aureus* phagocytosis, consistent with our observations above with mouse neutrophils. In contrast, both the accumulation of PtdIns3P on *S. aureus*-containing phagosomes and the rate of intracellular ROS production were similarly and substantially sensitive to inhibition by wortmannin, suggesting they may both be equivalently dependent on PI3K activity (Figure 6).

$p40^{phoxR58A/-}$ mice are defective in clearance of peritoneal S. aureus in vivo

Previous studies have defined an important role for the NADPH oxidase in the killing of *S. aureus in vitro* and *in vivo*, consistent with the prevalence of *S. aureus* infections in cases of CGD (Meischl and Roos, 1998; Heyworth *et al*, 2003; Rada *et al*, 2004). We investigated the ability of $p40^{phoxR58A/-}$ and $p40^{phox+/-}$ neutrophils to kill *S. aureus* in suspension cultures *in vitro* and to clear intraperitoneal injection of *S. aureus in vivo*. We have previously observed a severe defect in the ability of $p40^{phox-/-}$ neutrophils and $p40^{phox-/-}$ mice to kill *S. aureus* in these assays (Ellson *et al*, 2006). We observed a small but significant defect in the ability of $p40^{phoxR58A/-}$ neutrophils to kill *S. aureus in vitro* (Figure 7A). This defect was only a relatively small proportion (approx. 20%) of the total oxidase-dependancy of *S. aureus* killing in these assays (revealed by comparison with the NADPH oxidase inhibitor DPI; Figure 7A). However, this is consistent, given the nonlinear relationship between ROS production and *S. aureus* killing (Rada *et al*, 2004), with the relative sizes of the reductions in ROS production observed in $p40^{phoxR58A/-}$ and $p40^{phox-/-}$ neutrophils (Ellson *et al*, 2006). We also observed a highly significant defect in the ability of $p40^{phoxR58A/-}$ mice to clear a *S. aureus* infection *in vivo* (Figure 7B), demonstrating the physiological importance of an intact PX domain for NADPH function.

Discussion

Our observation that most $p40^{phoxR58A/R58A}$ embryos die early in development is very surprising. Mice lacking $gp91^{phox}$, $p47^{phox}$ or, indeed, $p40^{phox}$ are born in the expected

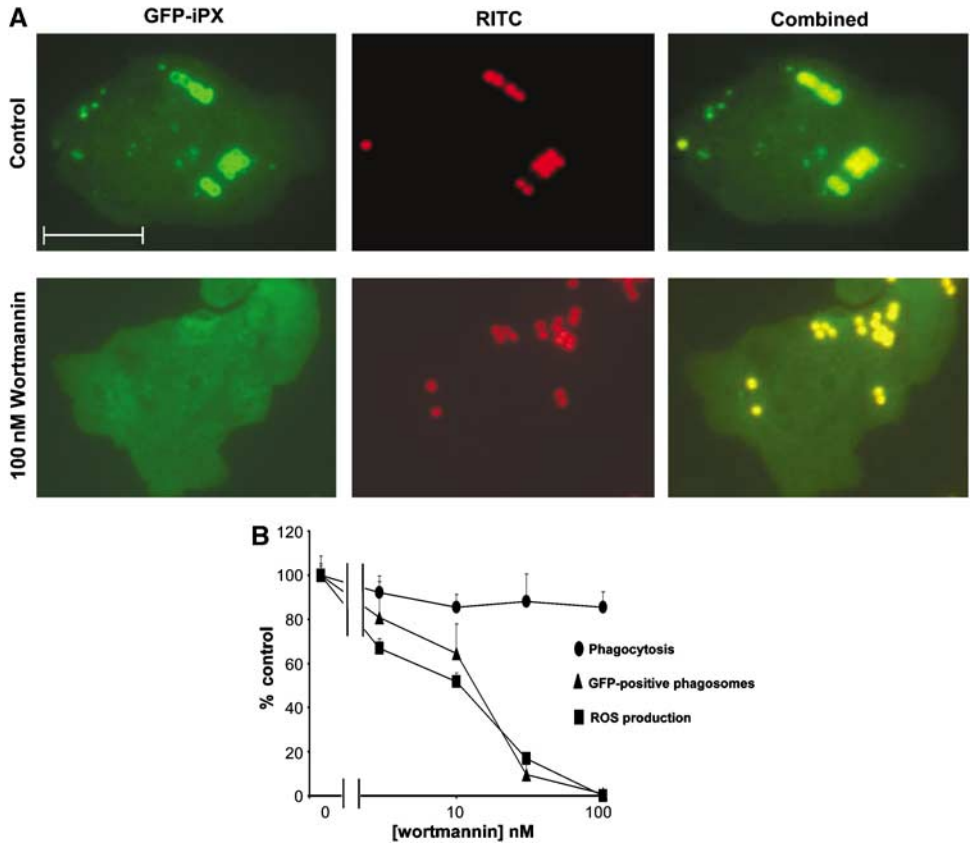

Figure 6 PtdIns3P accumulation and NADPH oxidase activation in response to *S. aureus* are inhibited in parallel by wortmannin. (**A**) 5×10^4 differentiated GFP-iPX PLB-985 cells were pretreated with DMSO (vehicle control) or 100 nM wortmannin prior to incubation with RITC-labelled, serum-opsonised *S. aureus* for 5 min. Samples were cytospun onto glass slides, fixed and mounted, and GFP-positive phagosomes and phagocytosed bacteria visualised by fluorescence microscopy; the scale bar represents 1 μm. (**B**) Intracellular ROS production in response to *S. aureus*, enumeration of GFP-positive phagosomes encapsulating phagocytosed *S. aureus*, and number of phagocytosed *S. aureus*/cell, in the presence of the indicated wortmannin concentrations, are expressed as a percentage of the relevant control (DMSO) responses. The wortmannin insensitive component of ROS production (approximately 22%) was subtracted from the ROS responses shown; data are means ± s.e., $n = 6$. Data for phagocytic indices are means ± s.e.; at least 60 cells were analysed for each condition.

Mendelian ratios (Jackson *et al*, 1995; Pollock *et al*, 1995; Ellson *et al*, 2006). This suggests that the $p40^{phoxR58A}$ allele has a lethal 'gain of function'. Further, our observation that $p40^{phoxR58A/-}$ animals are viable suggests that expression from both alleles is required to achieve a lethal threshold of R58A-$p40^{phox}$ protein. There are no previous reports of NADPH oxidase function during early embryogenesis, and there are no previous indications as to why high expression of R58A-$p40^{phox}$ would be lethal. The crystal structure of the PX domain of $p40^{phox}$ gives no clues as to how the R58A mutation might cause a significant change to the fold of $p40^{phox}$ (Bravo *et al*, 2001). Indeed, comparison of NADPH oxidase activity and the expression levels of oxidase subunits in $p40^{phoxR58A/-}$, $p40^{phox+/-}$ and $p40^{phox-/-}$ mice indicates R58A-$p40^{phox}$ is expressed at similar levels to wild-type protein, is correctly folded and is able to bind functionally to $p67^{phox}$. Heterologous expression of oxidase subunits in PLB-985 cells also confirms that R58A-$p40^{phox}$ and wild type protein can bind equivalently to $p67^{phox}$ (data not shown). Further work is clearly needed to clarify this effect of R58A-$p40^{phox}$ during embryo development, including its dependency on NADPH oxidase activity.

The production of fully differentiated neutrophils in $p40^{phoxR58A/-}$ mice and the normal expression of oxidase subunits in these cells compared to $p40^{phox+/-}$ neutrophils allow a direct comparison of $p40^{phoxR58A}$ and $p40^{phox}$ alleles and the potential to ascribe differences in neutrophil NADPH oxidase activity to the function of the PX domain in $p40^{phox}$. We observed large reductions in intracellular ROS production in response to *S. aureus* and IgG-latex beads but much smaller reductions in extracellular ROS produced in response to TNFα/fMLP. A comparison of the scale of these reductions with those we observed in equivalent oxidase responses in $p40^{phox-/-}$ neutrophils suggests that the larger defects in ROS production seen in $p40^{phox-/-}$ neutrophils, particularly extracellular ROS in response to TNF/fMLP and PMA (75 versus 25%, 80 versus −5%, for $p40^{phox-/-}$ versus $p40^{phoxR58A/-}$, respectively) may be caused by the loss of a non-PtdIns3P-binding function of $p40^{phox}$ or the significant decrease in $p67^{phox}$ expression in these cells (Ellson *et al*, 2006).

Given the clarity, both with which PtdIns3P is defined as a ligand for the PX domain of $p40^{phox}$ and with which the R58A mutation abolishes this binding, our observations start to define the contribution that PtdIns3P binding could, in principle, make to the role of $p40^{phox}$ in NADPH oxidase regulation. We measured a large reduction in intracellular ROS production in response to phagocytosis of *S. aureus* in the $p40^{phoxR58A/-}$ neutrophils. Importantly, this reduction overlapped substantially with the inhibition of a large element of this response by the general PI3K inhibitor wortmannin.

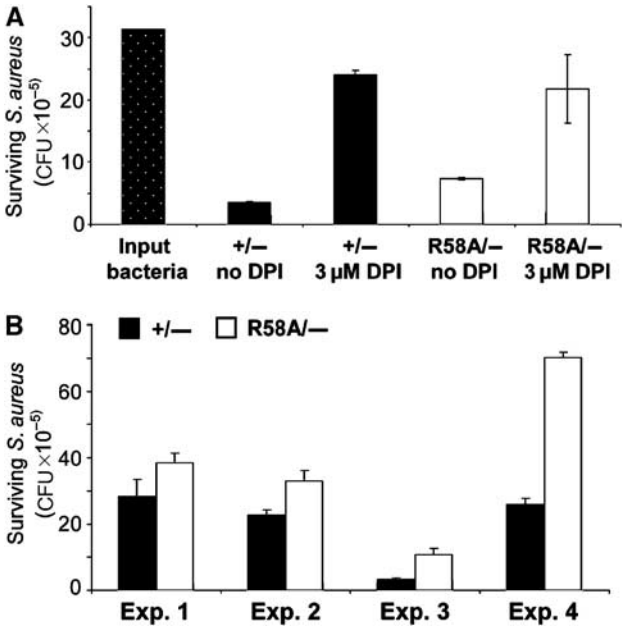

Figure 7 p40$^{phox R58A/-}$ neutrophils are deficient in killing of *S. aureus in vitro* and *in vivo*. (**A**) Primed BMNs from p40$^{phox R58A/-}$ and $^{+/-}$ animals were incubated with serum-opsonised *S. aureus* (approximate ratio of 1 bacterium to 4 neutrophils), in the presence or absence of 3 μM DPI, with rapid mixing. After 15 min, the neutrophils were lysed and surviving bacteria were counted. A control with no neutrophils (input bacteria) is included. Data are means ± s.e. ($n = 3$) and are representative of 2–5 experiments, using 3–6 mice per preparation. (**B**) Mice were injected intraperitoneally with approximately 5×10^7 live *S. aureus*. After 4 or 24 h, mice were killed, their peritoneums were flushed and surviving bacteria enumerated. Total numbers of surviving bacteria in four independent experiments are shown for the 4 h time point only; data are means ± s.e. ($n = 3$ mice per experiment). Two two-way analyses of variance were carried out on the data (one for the data at 4 h and one for the data at 24 h) to test whether the observed differences in bacterial survival were significant, taking into account the variability between the four experiments. The increased survival of *S. aureus* in the p40$^{phox R58A/-}$ mice was significant at 4 h ($F = 7.664$, $df = 3$, $P < 0.0001$) and 24 h ($F = 717.700$, $df = 3$, $P < 0.0001$).

Previous work has described an accumulation of the PI3K product, PtdIns3P, in phagosomes containing bacterial and IgG-opsonised targets in macrophage-like cell lines (Ellson *et al*, 2001b; Vieira *et al*, 2001). In agreement with the concept that PtdIns3P synthesis may be a general phenomenon associated with phagocytosis, we also observed intense PtdIns3P accumulation around *S. aureus*-containing phagosomes in differentiated PLB-985 cells. Inhibition of this PtdIns3P-accumulation by wortmannin correlated well with inhibition of *S. aureus*-induced intracellular ROS production, suggesting the two events may be causally linked. The source of PtdIns3P accumulation around these phagosomes is uncertain but previous data have suggested that a type III PI3K is essential for PtdIns3P accumulation in IgG-latex bead containing phagosomes (Vieira *et al*, 2001), which is consistent with the bulk of the wortmannin-sensitivity we have observed for the oxidase responses to *S. aureus* in both PLB-985 cells and mouse neutrophils. Taken together, these results form a powerful argument that PtdIns3P-binding to p40^{phox} is required to support over half the intracellular ROS production in *S. aureus* phagosomes, under the conditions studied. This does not preclude the possibility that PtdIns3P plays additional roles in oxidase regulation but does define, for the first time, the critical importance of the PtdIns3P:p40^{phox} PX domain interaction for the physiological regulation of the oxidase complex. This conclusion is in good agreement with the results of a recent study, which used a Cos-cell heterologous-expression system (COS^{phox}) to define the importance of the PX domain of p40^{phox} in regulating NADPH oxidase activation on IgG/SRBC-containing phagosomes (Suh *et al*, 2006). The molecular consequences of PtdIns3P binding to the PX domain of p40^{phox} are still unknown. It is not yet clear the degree to which this interaction is responsible for governing the membrane localisation of p40^{phox}, and its binding partner p67^{phox}, and/or an allosteric consequence in p40^{phox} which affects its interaction with other proteins, such as the other oxidase subunits.

The R58A mutation in p40^{phox} had a much larger ablatory effect on intracellular versus extracellular accumulation of ROS in response to PMA. This observation aligns with previous work, confirmed here, indicating that the smaller, intracellular ROS response is sensitive to inhibition by wortmannin, whereas the larger, extracellular ROS response is not (Karlsson *et al*, 2000). The idea that intracellular ROS accumulation in response to PMA is regulated by PtdIns3P is also in agreement with the dependency of this response on p40^{phox} in a cell-permeable, reconstitution model of oxidase activation (Brown *et al*, 2003). We also observed a small but significant sensitivity of TNF/fMLP-induced ROS to the R58A mutation. As described above, the rise in PtdIns3P around the phagosome correlates with its involvement in NADPH oxidase regulation at this membrane location. However, significant rises in PtdIns3P, which are coincident in time with oxidase activation, have not been observed in neutrophils stimulated by PMA or TNF/fMLP. This raises the question of whether oxidase-relevant rises in PtdIns3P are so small in response to these agonists that they have evaded detection or that the oxidase assembles on existing PtdIns3P-rich structures (Kobayashi *et al*, 1998; Karlsson *et al*, 2000), such as components or derivatives of the endosomal/lysosomal compartments.

The large defect in the *S. aureus*-induced oxidase response in neutrophils from p40$^{phox R58A/-}$ mice translated into a smaller defect in the *in vitro* killing of this organism. This is not surprising given previously established relationships between oxidase activity and *in vitro* killing of *S. aureus* by neutrophils (Rada *et al*, 2004). We did, however, observe a significant defect in the clearance of *S. aureus in vivo* in p40$^{phox R58A/-}$ animals. These experiments are limited to single modes of bacterial delivery, single doses of bacteria and limited times of sampling, and thus give only a small 'snapshot' of how these animals may deal with bacterial infections. They do however provide very strong evidence that the PtdIns3P:PX domain interaction in p40^{phox} has a significant physiological role in the regulation of NADPH oxidase activity and provide a basis for future work aimed at a more comprehensive evaluation of this signalling element in NADPH oxidase function.

Materials and methods

Murine GM-CSF (mGM-CSF), fMLP, luminol, DPI, PMA, HRP were from Sigma. Murine TNFα (mTNFα) was from R&D. Cell culture

reagents were from Invitrogen. All buffer components were from Sigma and were endotoxin-free or low endotoxin. Mouse serum was prepared as previously described (Ellson *et al*, 2006).

Generation of p40$^{phoxR58A/-}$ mice

Several clones encoding p40^{phox} genomic sequence were isolated from the RPCI mouse PAC library 21 (Pieter de Jong: UK HGMP Resource Centre) by Southern screens using an NT-cDNA probe. An 11.9 kb *Spe*I–*Spe*I fragment encompassing exons 1–4 was isolated from clone RP21-641C7 and inserted into the low copy number plasmid pSC-3Z to form the basis of a p40^{phox} gene-targeting vector (Figure 1A).

A smaller fragment containing exon 3 was subcloned into pBS; site-directed mutagenesis was conducted to alter codon 58 from CGC to GCC, altering the coded amino acid from arginine to alanine and an additional silent mutation to introduce a new *Xho*I site (Figure 1B), which was used to track the presence of the mutated sequence. This modified segment was sequenced and then re-introduced into the targeting vector.

A loxP-flanked cassette containing a tACE-Cre expression module and a Neo^{R} expression module (pACN; A. Plagge, Babraham Institute; Bunting *et al*, 1999) was inserted into the SnaBI site in the intron between exons 3–4 (Figure 1A). The tACE promoter is expected to operate in the testis and to drive Cre/Lox mediated deletion of this cassette on breeding of targeted chimeras; deletion is predicted to leave 59 bp of foreign DNA remaining in the intron.

The final targeting vector was digested with *Dra*I and *Sal*I (in the 3′ polylinker) to remove excess pSC-3Z vector sequence and used to transfect E14 129$^{s/v}$ ES cells by the Gene Targeting Facility, Babraham Institute. Four hundred and eighty clones were initially screened for homologous recombination using a 3′-Southern screen (probe 3′ to targeted sequence, *Eco*RI digest, 4.6–8.3 kb transition) and positive clones re-screened by a 5′-Southern (probe 5′ to targeted sequence, *Spe*I digest, 11.9–10.0 kb transition) and for single insertion of the Neo^{R} cassette (Neo probe, *Eco*RI/8.3 kb and *Spe*I/5.7 kb) (Figure 1C). Two clones were taken forward for blastocyst injection and male chimeras from these mice were bred with female C57$^{BL/6}$ animals to generate p40$^{phoxR58A/+}$ heterozygotes on a mixed 129$^{s/v}$/C57$^{BL/6}$ background. Deletion of the Neo^{R} cassette was confirmed by appropriate Southern and PCR analysis and separate p40$^{phoxR58A/+}$ colonies were created from each of the original targeted ES cell lines and housed under specific pathogen-free conditions in the SABU facility at the Babraham Institute. Genotyping of the mice was performed by PCR amplification of an approximately 850 bp region flanking exon 3 (to include the additional *Xho*I site) and subsequent diagnosis by susceptibility of the product to cleavage by *Xho*I (to yield approximately 525 and 325 bp fragments) (Figure 1D). All mice used were 2–8 months old and showed no age-dependent variation. This work was covered by UK Home Office Project Licence PPL 80/1875.

Preparation of bone marrow-derived neutrophils

BMNs were prepared as previously described with minor modifications (Condliffe *et al*, 2005). Bone marrow, from 2 to 3 mice per preparation, was dispersed in HBSS (without Ca^{2+} and Mg^{2+}), 0.25% fatty acid-free BSA, 15 mM HEPES pH 7.4 RT and purified over discontinuous Percoll (Amersham) gradients. Following washes, mature neutrophils were resuspended in Dulbecco's PBS with Ca^{2+} and Mg^{2+}, 1 g/l glucose, 4 mM sodium bicarbonate (DPBS+). Purity was typically 70–80% assessed by cytospin and REASTAIN Quick-Diff (Reagena, Finland) staining. All assays were carried out in DPBS+. BMNs were primed at 37°C with 500 U/ml mTNFα and 100 ng/ml mGM-CSF for 60 min. In some experiments, as indicated, BMNs were primed with 500 U/ml mTNFα alone for 30 min.

Blood cell counts in p40$^{phoxR58A/-}$ mice

Peripheral blood from p40$^{phoxR58A/-}$ and $^{+/-}$ control animals was collected into Microvette EDTA blood collection tubes (Sarstedt) and analysed in a Vetabc animal blood cell counter to determine the relative cell types.

Neutrophil Western blots

5×10^6 BMNs were sonicated into 1× SDS loading buffer and 5×10^5 cell equivalents were subjected to SDS–PAGE, transferred and blotted for p40^{phox} (Upstate, 05–539), p47^{phox} (Upstate, 07–500) and p67^{phox} (Upstate, 07–502). Enhanced chemiluminescence signal was detected (Image Reader LAS-1000, Fugifilm) and quantified using Aida Image Analyser 2.2.

Cell culture

PLB-985s stably expressing GFP-iPX were maintained in RPMI 1640 media containing L-Glutamine and supplemented with 10% heat-inactivated foetal bovine serum, 100 U/ml penicillin and 100 μg/ml streptomycin at 37°C in a 5% CO_2 humidified atmosphere. Cells were differentiated by addition of 0.5% *N*,*N*-dimethylformamide to cell media and changing media every second day for 6 days. Prior to ROS/phagocytosis assays, cells were pelleted and resuspended in DPBS+.

Chemiluminescent detection of ROS

ROS production by BMNs and PLB985 cells (3.75×10^5/well) was measured by luminol-dependent chemiluminescence in a multiplate luminometer, as described previously (Ellson *et al*, 2006). Assays were conducted in the presence or absence of exogenously added HRP (18.75 U/ml) to measure extracellular or intracellular ROS, respectively. fMLP was used at 10 μM, PMA at 300 nM and IgG-latex beads and serum-opsonised *S. aureus* were used at BMN:particle ratios of 1:50 and 1:20, respectively. Where appropriate, BMNs were preincubated with the indicated concentrations of wortmannin for 10 min prior to addition of stimuli. Data output is in relative light units per second (rlu/s) or total rlu integrated over the indicated periods of time.

Preparation of particulate stimuli

Carboxylate-modified latex beads (0.9 μm diameter) were cross-linked to sulphydryl-modified BSA and coated with an anti-BSA monoclonal antibody, as previously described (Cox *et al*, 1999) (IgG-latex beads). *S. aureus* were serum-opsonised by incubation in DPBS+ with 10% mouse serum at 37°C with end-over-end mixing for 15 min followed by washing.

S. aureus phagocytosis assay

5×10^4 primed BMNs or differentiated GFP-iPX expressing PLB-985s were incubated in suspension at 37°C with 1×10^6 RITC-labelled, serum-opsonised *S. aureus* (Rooijakkers *et al*, 2005). After 5 min (PLB-985) or 30 min (BMN), samples were cytospun onto glass slides and fixed in 100% methanol containing 0.01% methylene-blue. In some experiments, samples were placed on ice for 5 min, to prevent further phagocytosis, and non-phagocytosed RITC-labelled *S. aureus* quenched with trypan blue (1.2 mg/ml), prior to cytospinning. Coverslips were placed over samples with Aqua-Polymount anti-fading solution (Poly-Science Inc) and GFP-positive phagosomes (PLB-985s) and phagocytosed bacteria were visualised by fluorescence microscopy and enumerated.

In vitro bacterial killing assays

Bacteria (*S. aureus* Wood 46) were subcultured at 37°C to logarithmic growth from an overnight culture. 4×10^7 bacteria were washed in DPBS+, and opsonised as detailed above. Opsonised bacteria (1.5×10^6) were added to 6.2×10^6 primed BMNs (2.5×10^7/ml) at 37°C with rapid orbital mixing. At the indicated times, 50 μl aliquots were removed to 950 μl ice-cold Luria Broth (LB) containing 0.05% saponin. Samples were sonicated (Misonix, Sonicator 3000, output 1.5, 10 s) to liberate intracellular bacteria and returned to ice. Suspensions were serially diluted and plated on LB-agar to enumerate surviving bacteria. In some experiments, neutrophils were incubated for 5 min with 3 μM DPI or vehicle (DMSO) alone, prior to the addition of bacteria.

In vivo S. aureus survival assays

S. aureus (LS-1) were subcultured at 37°C to logarithmic growth from an overnight culture. Bacteria were washed and resuspended in injection-grade PBS at 2.5×10^8/ml. Three animals of each genotype per timepoint were injected intraperitoneally with 0.2 ml of bacterial suspension (5×10^7 bacteria). After 4 or 24 h, mice were killed and the peritoneal cavity was thoroughly flushed with 10 ml ice-cold PBS, 5 mM EDTA, 5 U/ml heparin. Aliquots were diluted, sonicated, plated and bacteria were enumerated as for the *in vitro* killing assays.

Acknowledgements

We thank Ted Saunders, Martin George and Debbie Drage of the Gene Targeting Facility at Babraham for their excellent support; Anne Segonds-Pichon for statistical analysis; members of the Small Animal Breeding Unit at Babraham for animal husbandry and the laboratory of Anthony Green (Department of Haematology, Cambridge University) for use of their animal blood cell counter. This work was supported by grants from the BBSRC and Arthritis Research Council (S0679). CDE is a Beit Memorial Fellow. The authors have no conflicting financial interests.

References

Ago T, Takeya R, Hiroaki H, Kuribayashi F, Ito T, Kohda D, Sumimoto H (2001) The PX domain as a novel phosphoinositide-binding molecule. *Biochem Biophys Res Commun* **287:** 733–738

Bey EA, Xu B, Bhattacharjee A, Oldfield CM, Zhao X, Li Q, Subbulakshmi V, Feldman GM, Wientjes FB, Cathcart MK (2004) Protein kinase C delta is required for p47phox phosphorylation and translocation in activated human monocytes. *J Immunol* **173:** 5730–5738

Bravo J, Karathanassis D, Pacold CM, Pacold ME, Ellson CD, Anderson KE, Butler PJ, Lavenir I, Perisic O, Hawkins PT, Stephens L, Williams RL (2001) The crystal structure of the PX domain of $p40^{Phox}$ bound to phosphatidylinositiol 3-phosphate. *Mol Cell* **8:** 829–839

Brown GE, Stewart MQ, Liu H, Ha VL, Yaffe MB (2003) A novel assay system implicates PtdIns(3,4)P(2), PtdIns(3)P, and PKC delta in intracellular production of reactive oxygen species by the NADPH oxidase. *Mol Cell* **11:** 35–47

Bunting M, Bernstein KE, Greer JM, Capecchi MR, Thomas KR (1999) Targeting genes for self-excision in the germ line. *Genes Dev* **13:** 1524–1528

Condliffe AM, Davidson K, Anderson KE, Ellson CD, Crabbe T, Okkenhaug K, Vanhaesebroeck B, Turner M, Webb L, Wymann MP, Hirsch E, Ruckle T, Camps M, Rommel C, Jackson SP, Chilvers ER, Stephens LR, Hawkins PT (2005) Sequential activation of class IB and class IA PI3K is important for the primed respiratory burst of human but not murine neutrophils. *Blood* **106:** 1432–1440

Cox D, Tseng CC, Bjekic G, Greenberg S (1999) A requirement for phosphatidylinositol 3-kinase in pseudopod extension. *J Biol Chem* **274:** 1240–1247

Cross AR, Segal AW (2004) The NADPH oxidase of professional phagocytes-prototype of the NOX electron transport chain systems. *Biochim Biophys Acta* **1657:** 1–22

Dahlgren C, Karlsson A (1999) Respiratory burst in human neutrophils. *J Immunol Methods* **232:** 3–14

Dang PM, Fontayne A, Hakim J, El Benna J, Perianin A (2001) Protein kinase C zeta phosphorylates a subset of selective sites of the NADPH oxidase component p47phox and participates in formyl peptide-mediated neutrophils respiratory burst. *J Immunol* **166:** 1206–1213

Dekker LV, Leitges M, Altschuler G, Mistry N, McDermott A, Roes J, Segal AW (2000) Protein kinase C-beta contributes to NADPH oxidase activation in neutrophils. *Biochem J* **347:** 285–289

Diebold BA, Bokoch GM (2001) Molecular basis for Rac2 regulation of phagocyte NADPH oxidase. *Nat Immunol* **2:** 211–215

Dinauer MC (2003) Regulation of neutrophil function by Rac GTPases. *Curr Opin Hematol* **10:** 8–15

Dong X, Mo Z, Bokoch G, Guo C, Li Z, Wu D (2005) P-Rex1 is a primary Rac2 guanine nucleotide exchange factor in mouse neutrophils. *Curr Biol* **15:** 1874–1879

Ellson CD, Gobert-Gosse S, Anderson KE, Davidson K, Erdjument-Bromage H, Tempst P, Thuring JW, Cooper MA, Lim ZY, Holmes AB, Gaffney PR, Coadwell J, Chilvers ER, Hawkins PT, Stephens LR (2001a) PtdIns(3)P regulates the neutrophil oxidase complex by binding to the PX domain of p40(phox). *Nat Cell Biol* **3:** 679–682

Ellson CD, Anderson KE, Morgan G, Chilvers ER, Lipp P, Stephens LR, Hawkins PT (2001b) Phosphatidylinositol 3-phosphate is generated in phagosomal membranes. *Curr Biol* **11:** 1631–1635

Ellson CD, Davidson K, Ferguson GJ, O'Connor R, Stephens LR, Hawkins PT (2006) Neutrophils from $p40^{phox-/-}$ mice exhibit severe defects in NADPH oxidase regulation and oxidant-dependent bacterial killing. *J Exp Med* **203:** 1927–1937

Faust LP, el Benna J, Babior BM, Chanock SJ (1995) The phosphorylation targets of $p47^{Phox}$, a subunit of the respiratory burst oxidase. Functions of the individual target serines as evaluated by site-directed mutagenesis. *J Clin Invest* **96:** 1499–1505

Fontayne A, Dang PM, Gougerot-Pocidalo MA, El-Benna J (2002) Phosphorylation of p47phox sites by PKC alpha, beta II, delta, and zeta: effect on binding to p22phox and on NADPH oxidase activation. *Biochemistry* **41:** 7743–7750

Groemping Y, Rittinger K (2005) Activation and assembly of the NADPH oxidase: a structural perspective. *Biochem J* **386:** 401–416

Hallett MB, Lloyds D (1995) Neutrophil priming: the cellular signals that say 'amber' but not 'green'. *Immunol Today* **16:** 264–268

Hampton MB, Kettle AJ, Winterbourn CC (1998) Inside the neutrophil phagosome: oxidants, myeloperoxidase, and bacterial killing. *Blood* **92:** 3007–3017

Heyworth PG, Cross AR, Curnutte JT (2003) Chronic granulomatous disease. *Curr Opin Immunol* **15:** 578–584

Jackson SH, Gallin JI, Holland SM (1995) The p47phox mouse knock-out model of chronic granulomatous disease. *J Exp Med* **182:** 751–758

Jakus Z, Berton G, Ligeti E, Lowell CA, Mocsai A (2004) Responses of neutrophils to anti-integrin antibodies depends on costimulation through low affinity Fc-gammaRs: full activation requires both integrin and nonintegrin signals. *J Immunol* **173:** 2068–2077

Kanai F, Liu H, Field SJ, Akbary H, Matsuo T, Brown GE, Cantley LC, Yaffe MB (2001) The PX domains of p47phox and p40phox bind to lipid products of PI(3)K. *Nat Cell Biol* **3:** 675–678

Karathanassis D, Stahelin RV, Bravo J, Perisic O, Pacold CM, Cho W, Williams RL (2002) Binding of the PX domain of p47(phox) to phosphatidylinositol 3,4-bisphosphate and phosphatidic acid is masked by an intramolecular interaction. *EMBO J* **21:** 5057–5068

Karlsson A, Nixon JB, McPhail LC (2000) Phorbol myristate acetate induces neutrophil NADPH-oxidase activity by two separate signal transduction pathways: dependent or independent of phosphatidylinositol 3-kinase. *J Leukoc Biol* **67:** 396–404

Knight ZA, Gonzalez B, Feldman ME, Zunder ER, Goldenberg DD, Williams O, Loewith R, Stokoe D, Balla A, Toth B, Balla T, Weiss WA, Williams RL, Shokat RL (2006) A pharmacological map of the PI3-K family defines a role for p110α in insulin signalling. *Cell* **125:** 733–747

Kobayashi T, Robinson JM, Seguchi H (1998) Identification of intracellular sites of superoxide production in stimulated neutrophils. *J Cell Sci* **111:** 81–91

Lapouge K, Smith SJM, Walker PA, Gamblin SJ, Smerdon SJ, Rittinger K (2000) Structure of the TPR domain of $p67^{phox}$ in complex with Rac-GTP. *Mol Cell* **6:** 899–907

Matute JD, Arias AA, Dinauer MC, Patino PJ (2005) $p40^{Phox}$: The last NADPH oxidase subunit. *Blood Cells Mol Dis* **35:** 291–302

Meischl C, Roos D (1998) The molecular basis of chronic granulomatous disease. *Springer Semin Immunopathol* **19:** 417–434

Murphy R, DeCoursey TE (2006) Charge compensation during the phagocyte respiratory burst. *Biochim Biophys Acta* (in press) http://dx.doi.org/10.1016/j.bbabio.2006.01.005

Nathan C (2006) Neutrophils and immunity; challenges and opportunities. *Nat Rev Immun* **6:** 173–182

Perisic O, Wilson MI, Karathanassis D, Bravo J, Pacold ME, Ellson CD, Hawkins PT, Stephens L, Williams RL (2004) The role of phosphoinositides and phosphorylation in regulation of NADPH oxidase. *Adv Enzyme Regul* **44:** 279–298

Pollock JD, Williams DA, Gifford MA, Li LL, Du X, Fisherman J, Orkin SH, Doerschuk CM, Dinauer MC (1995) Mouse model of X-linked chronic granulomatous disease, an inherited defect in phagocyte superoxide production. *Nat Genet* **9:** 202–209

Quinn MT, Gauss KA (2004) Structure and regulation of the neutrophil respiratory burst oxidase: comparison with nonphagocyte oxidases. *J Leukoc Biol* **76:** 760–781

Rada BK, Geiszt M, Kaldi K, Timar C, Ligeti E (2004) Dual role of phagocytic NADPH oxidase in bacterial killing. *Blood* **104:** 2947–2953

Reeves EP, Lu H, Jacobs HL, Messina CG, Bolsover S, Gabella G, Potma EO, Warley A, Roes J, Segal AW (2002) Killing activity of neutrophils is mediated through activation of proteases by K+ flux. *Nature* **416:** 291–297

Rooijakkers SH, van Wamel WJ, Ruyken M, van Kessel KP, van Strijp JA (2005) Anti-opsonic properties of staphylokinase. *Microbes Infect* **7:** 476–484

Sheppard FR, Kelher MR, Moore EE, McLaughlin NJ, Banerjee A, Silliman CC (2005) Structural organization of the neutrophil NADPH oxidase: phosphorylation and translocation during priming and activation. *J Leukoc Biol* **78:** 1025–1042

Stephens L, Cooke FT, Walters R, Jackson T, Volinia S, Gout I, Waterfield MD, Hawkins PT (1994) Characterization of a phosphatidylinositol-specific phosphoinositide 3-kinase from mammalian cells. *Curr Biol* **4:** 203–214

Suh C-I, Stull ND, Li XJ, Tian W, Price MO, Grinstein S, Yaffe MB, Atkinson S, Dinauer MC (2006) The phosphoinositide-binding protein $p40^{phox}$ activates the NADPH oxidase during FcγIIa receptor-induced phagocytosis. *J Exp Med* **203:** 1915–1925

Ueyama T, Lennartz MR, Noda Y, Kobayashi T, Shirai Y, Rikitake K, Yamasaki T, Hayashi S, Sakai N, Seguchi H, Sawada M, Sumimoto H, Saito N (2004) Superoxide production at phagosomal cup/phagosome through beta I protein kinase C during Fc gamma R-mediated phagocytosis in microglia. *J Immunol* **173:** 4582–4589

Vieira OV, Botelho RJ, Rameh L, Brachmann SM, Matsuo T, Davidson HW, Schreiber A, Backer JM, Cantley LC, Grinstein S (2001) Distinct roles of class I and class III phosphatidylinositol 3-kinases in phagosome formation and maturation. *J Cell Biol* **155:** 19–25

Welch HC, Coadwell WJ, Stephens LR, Hawkins PT (2003) Phosphoinositide 3-kinase-dependent activation of Rac. *FEBS Lett* **546:** 93–97

Welch HC, Condliffe AM, Milne LJ, Ferguson GJ, Hill K, Webb LM, Okkenhaug K, Coadwell WJ, Andrews SR, Thelen M, Jones GE, Hawkins PT, Stephens LR (2005) P-Rex1 regulates neutrophil function. *Curr Biol* **15:** 1867–1873

Zhan Y, Virabasius JV, Song X, Pomerleau DP, Zhou GW (2002) The $p40^{phox}$ and $p47^{phox}$ PX domains of NADPH oxidase target cell membranes via direct and indirect recruitment by phosphoinositides. *J Biol Cell* **277:** 4512–4518

Zhou MJ, Brown EJ (1994) CR3 (Mac-1, alpha M beta 2, CD11b/CD18) and Fc gamma RIII cooperate in generation of a neutrophil respiratory burst: requirement for Fc gamma RIII and tyrosine phosphorylation. *J Cell Biol* **125:** 1407–1416

